Received: 20 July 2017 | Accepted: 1 December 2017

DOI: 10.1111/pce.13121

ORIGINAL ARTICLE

WILEY Plant, Cell & Environment

Co-occurring woody species have diverse hydraulic strategies and mortality rates during an extreme drought

Daniel M. Johnson[1] | Jean-Christophe Domec[2,3] | Z. Carter Berry[1,4] | Amanda M. Schwantes[3] | Katherine A. McCulloh[5] | David R. Woodruff[6] | H. Wayne Polley[7] | Remí Wortemann[8] | Jennifer J. Swenson[3] | D. Scott Mackay[9] | Nate G. McDowell[10] | Robert B. Jackson[11]

[1] College of Natural Resources, University of Idaho, Moscow, ID 83844, USA

[2] Bordeaux Sciences Agro, UMR INRA-ISPA 1391, Gradignan 33195, France

[3] Nicholas School of the Environment, Duke University, Durham, NC 27708, USA

[4] Department of Natural Resources and the Environment, University of New Hampshire, Durham, NH 03824, USA

[5] Department of Botany, University of Wisconsin-Madison, Madison, WI 53705, USA

[6] US Forest Service, Pacific Northwest Research Station, Corvallis, OR 97331, USA

[7] Grassland, Soil & Water Research Laboratory USDA–Agricultural Research Service, Temple, TX 76502, USA

[8] INRA Nancy, UMR INRA-UL 1137 Ecologie et Ecophysiologie Forestières, Champenoux 54280, France

[9] Department of Geography, State University of New York, Buffalo, NY 14261, USA

[10] Pacific Northwest National Laboratory, Richland, WA 99352, USA

[11] Department of Earth System Science, Woods Institute for the Environment, and Precourt Institute for Energy, Stanford University, Stanford, CA 94305, USA

Correspondence
Daniel M. Johnson, College of Natural Resources, University of Idaho, Moscow, ID 83844, USA.
Email: danjohnson@uidaho.edu

Funding information
National Science Foundation, Division of Earth Sciences, Grant/Award Number: EAR-1344703; USDA National Institute of Food and Agriculture, Grant/Award Number: #2012-00857; National Science Foundation, Division of Integrative Organismal Systems, Grant/Award Numbers: IOS-1146746, IOS-1450679, IOS-1549971 and IOS-1557906

Abstract

From 2011 to 2013, Texas experienced its worst drought in recorded history. This event provided a unique natural experiment to assess species-specific responses to extreme drought and mortality of four co-occurring woody species: *Quercus fusiformis*, *Diospyros texana*, *Prosopis glandulosa*, and *Juniperus ashei*. We examined hypothesized mechanisms that could promote these species' diverse mortality patterns using postdrought measurements on surviving trees coupled to retrospective process modelling. The species exhibited a wide range of gas exchange responses, hydraulic strategies, and mortality rates. Multiple proposed indices of mortality mechanisms were inconsistent with the observed mortality patterns across species, including measures of the degree of iso/anisohydry, photosynthesis, carbohydrate depletion, and hydraulic safety margins. Large losses of spring and summer whole-tree conductance (driven by belowground losses of conductance) and shallower rooting depths were associated with species that exhibited greater mortality. Based on this retrospective analysis, we suggest that species more vulnerable to drought were more likely to have succumbed to hydraulic failure belowground.

KEYWORDS

carbon gain, cavitation, climate change, stomatal conductance, water relations

1 | INTRODUCTION

The loss of water that accompanies photosynthesis has been a constraint facing land plants throughout their evolutionary history (Beerling, 2008). Under current and near-future climatic conditions, we can expect warmer temperatures, greater vapour pressure deficits ($VPD_{LA;}$ McDowell & Allen, 2015) and more frequent and severe droughts (Allen, Breshears, & McDowell, 2015; Diffenbaugh, Swain, & Touma, 2015; Polley, Briske, Wolter, Bailey, & Brown, 2013; Trenberth et al., 2014) than experienced in the recent past. In fact,

current work suggests recent droughts in the United States are the most severe of the past ~1,200 years (Johnson, Sherrard, Domec, & Jackson, 2014; Griffin & Anchukaitis, 2014).

To survive extreme drought events, plants must manage the loss of water and uptake of carbon. Plant water and carbon management strategies that have been linked to drought tolerance include stomatal regulation of plant water potentials and the associated degree of isohydry (Garcia-Forner et al., 2016; McDowell et al., 2008; Skelton, West, & Dawson, 2015; Tardieu & Simonneau, 1998), tissue/organ and whole-plant resistance to hydraulic dysfunction (e.g., Johnson et al., 2016; Kolb & Davis, 1994; Linton, Sperry, & Williams, 1998) and associated hydraulic safety margins (Choat et al., 2012; Meinzer, Johnson, Lachenbruch, McCulloh, & Woodruff, 2009), rooting depth (Padilla & Pugnaire, 2007; Pinheiro, DaMatta, Chaves, Loureiro, & Ducatti, 2005), and carbon utilization and allocation patterns (McDowell, 2011; Mitchell et al., 2013). It remains unclear which aspects of drought tolerance and which physiological metrics will prove more useful in predicting drought-induced mortality.

During 2011–2013, central Texas experienced its worst drought since record-keeping began in 1895 and potentially in the past 1,200 years (Johnson et al., 2014; Kukowski, Schwinning, & Schwartz, 2013; Moore et al., 2016). This period had less than half of the normal rainfall, and maximum daily growing season temperatures were between 4 and 6 °C greater than average maximum daily growing season temperatures, resulting in afternoon VPD_{LA} >6 kPa. Approximately 300 million trees died during this drought in Texas and 100 million of those were in central Texas (Moore et al., 2016; Schwantes et al., 2017).

We used the 2011–2013 Texas drought event to measure and understand plant physiological parameters aboveground and belowground related to drought tolerance in four co-occurring species in central Texas. Additionally, we used a soil-plant-atmosphere process-based model (Terrestrial Regional Ecosystem Exchange Simulator [TREES]; Mackay et al., 2015) to predict physiological parameters that are proposed to have mechanistic relationships with drought-induced mortality. TREES is a mechanistic plant physiology-hydraulic model that was highly constrained by data collected in the field, and thus likely to produce accurate outputs (Mackay et al., 2015; Tai, Mackay, Anderegg, Sperry, & Brooks, 2017). Our approach was to use established frameworks of hydraulic safety (Choat et al., 2012), degree of isohydry (Skelton et al., 2015), water use envelope (Sperry, Adler, Campbell, & Comstock, 1998), and plant NSC concentrations (Sevanto, McDowell, Dickman, Pangle, & Pockman, 2014) to assess which framework was most consistent with plant mortality in this study system (Table 1). We hypothesized that a combination of hydraulic and carbon pool parameters representing the coupled nature of carbon starvation and hydraulic failure (McDowell, 2011; O'Brien, Leuzinger, Philipson, Tay, & Hector, 2014) would best explain the observed mortality.

2 | MATERIALS AND METHODS

2.1 | Measured canopy dieback and tree mortality

Canopy cover loss and post-drought live cover by species was measured on the ground in four sites across the Edwards Plateau region of Texas in July 2013. Twenty-one plots were sampled, with 3–6 plots at each of four sites as described in Schwantes, Swenson, and Jackson (2016). A stratified random sample was used to select plot locations. High-resolution orthophotos (1 m, near-infrared) from the National Agriculture Imagery Program predrought (2010) and postdrought (2012) were used to create tree canopy loss maps over each of the four sites. Then, three equal area strata were assigned categorically based on (high, med, and low) tree canopy loss observed in these canopy-loss maps. Within each of the three categories, 1–2 plot locations were randomly selected, for a total of 3–6 plots per site. This sampling procedure ensured that within a site, we sampled across the entire range of canopy loss, while every location still had the same probability of being sampled. Canopy mortality was distinguished from foliar loss due to drought deciduousness based on additional orthophotos taken in 2014 (Figure 1a).

For each plot, canopy cover (to the nearest 0.1 m) was measured along four 25-m transects running from plot centre in each of the four cardinal directions (N, E, S, and W) using the line-intercept method. In steep terrain, where slopes were greater than 5°, transect length was corrected for the incline. To measure the intersection of a woody shrub or tree's canopy cover and the measuring tape, we used a 2.5-m perpendicular metal sampling rod for shrubs/trees under 2.5 m. For shrubs/trees over 2.5 m, we used a GSR densitometer, a sighting device. Woody shrubs and trees under 1 m tall were not included in the field surveys.

2.2 | Study sites for physiological measurements

We used two research sites in the Edward's Plateau region (west–central Texas) for the current study. One was an established research site (Powell cave, see Jackson, Moore, Hoffmann, Pockman, & Linder, 1999; McElrone, Pockman, Martinez-Vilalta, & Jackson, 2004) in Menard, TX, USA, and the other was in Colorado Bend State Park near Bend, TX, USA. Both sites have karst topography with shallow soils (typically less than 20 cm; soil depths were confirmed by

TABLE 1 Predicted tree mortality mechanism frameworks assessed in the current study

Framework assessed	Measured or modelled	Consistent with mortality?
Hydraulic safety (as in Choat et al., 2012)	Measured	No
Degree of isohydry (as in Skelton et al., 2015)	Measured	No
Nonstructural carbohydrate concentrations (Sevanto et al., 2014)	Modelled	No
Water use envelope (Sperry et al., 1998)	Modelled	Yes
Photosynthesis and stomatal sensitivity to VPD	Measured	No

Note. VPD = vapour pressure deficit.

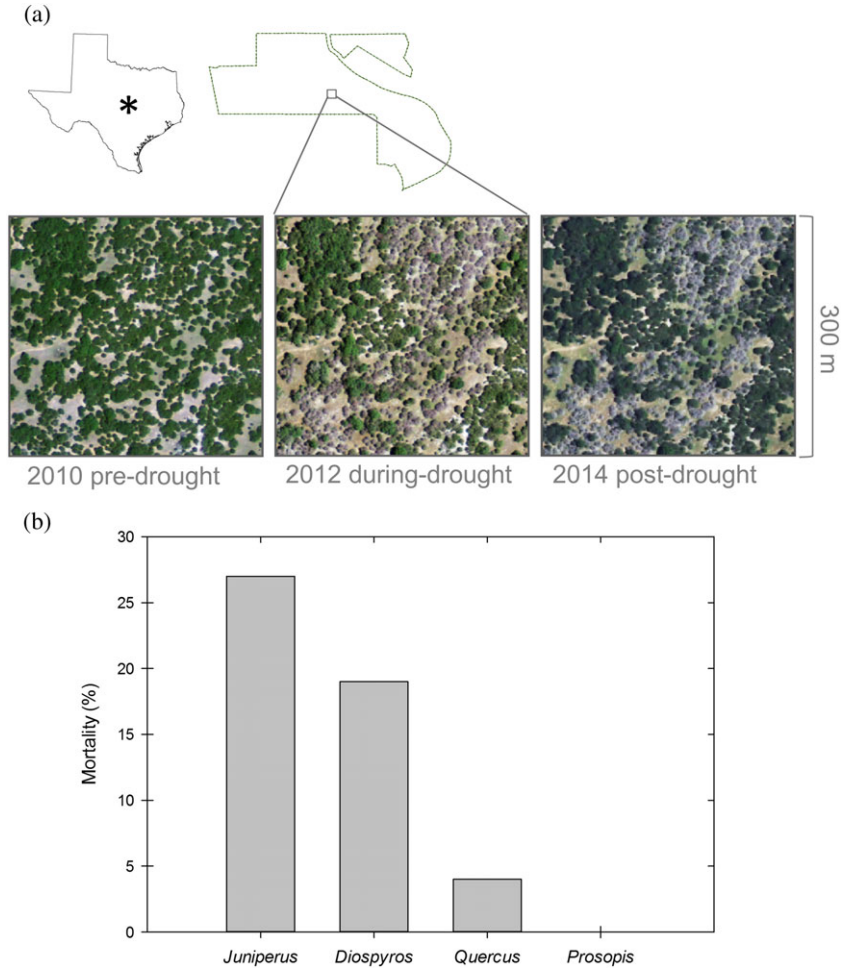

FIGURE 1 (a) Predrought (2010), during drought (2012), and postdrought (2014) 1-m orthophotos at Colorado Bend State Park showing that trees marked as dead did not produce new growth, as observed in the orthophotos (National Agriculture Imagery Program, available from the U.S. Geological Survey). (b) Percent observed mortality from 2013 transects, across the Edwards Plateau region of Texas

probing the bedrock using a metallic rod, and soils were <30 cm deep at all places tested at both sites) with underlying fractured limestone (see van Auken, Ford, Stein, & Stein, 1980; McElrone et al., 2004 for detailed site descriptions). Mean annual precipitation at these sites is approximately 700 mm and mean January and July temperatures are 8 and 27 °C, respectively. The four-dominant tree species studied were *Diospyros texana* Scheele, *Juniperus ashei* J. Buchholz, *Prosopis glandulosa* Torr., and *Quercus fusiformis* Small, with *Juniperus* absent at the Menard site (see Table 2 for species descriptions). The Menard site is an active cattle ranch where all *Juniperus* had been removed, which is common among managed cattle ranches in Texas (Thurow & Hester, 1997). Physiological measurements (see below) were performed on *Quercus*, *Prosopis*, and *Juniperus* at Colorado Bend and *Quercus*, *Prosopis* and *Diospyros* at Menard. Our objectives in using the two study sites were to increase our sample area, number of species, and individuals sampled. We also determined that three species per site was the number that we could measure effectively within a 60-min time period.

During the study period (May–September 2013), the study area was under a long-term drought (drought began in 2011, see Johnson et al., 2014; Moore et al., 2016; Schwantes et al., 2017). The most severe portion of the drought concluded in 2012; however, the U.S.

TABLE 2 Species, family, leaf habit, growth form, maximum height, maximum rooting depth, and minimum predawn leaf water potentials (measured in the 2013 growing season; numbers in parentheses are standard errors) for the four study species (from Flora of North America 1993+)

Species	Family	Leaf habit	Growth form	Maximum height (m)	Maximum rooting depth (m)[a]	Minimum predawn leaf water potential (MPa)
Diospyros texana Scheele	Ebenaceae	Winter deciduous	Multi-stemmed large shrub to small tree	15	8[b]	−2.6 (0.1)
Juniperus ashei J. Buchholz	Cupressaceae	Evergreen	Multi-stemmed large shrub to small tree	15	8	−5.7 (0.2)
Prosopis glandulosa Torr.	Fabaceae	Winter deciduous	Single-stemmed tree	15	18	−2.5 (0.2)
Quercus fusiformis Small	Fagaceae	Winter deciduous	Single-stemmed tree	25	22	−1.8 (0.1)

[a]From Jackson et al. (1999).

[b]No information for *Diospyros*, but it was assumed to have maximum rooting depth of 8 m or less.

Drought Monitor (droughtmonitor.unl.edu; National Drought Mitigation Center) reported the study area as category D2 (severe drought) or D3 (extreme drought) from April to mid-July 2013, and then a D1 category (moderate drought) from mid-July through the end of August 2013. This change in drought categorization was due to 12–15 cm of rainfall that occurred from July15 to 18, depending on the area (see Figure S1). The entire study area was under long-term drought (as defined by the National Drought Mitigation Center) for the entire study.

2.3 | Sampling for physiological measurements

Ten individuals, apparently healthy (i.e., no apparent canopy dieback) adult trees per species were identified and tagged at each site. These individuals were used for all physiological measurements, with each set of measurements (e.g., hourly gas exchange) performed on randomly selected individuals within the 10 selected trees. Six branch samples (one per tree for six trees) and six root samples (one per tree for six trees) were collected for each species at each site (*Quercus* and *Prosopis* measured at both sites and hydraulic parameters were not significantly different between sites). *Diospyros* was only collected from the Menard site and *Juniperus* was only collected from the Colorado Bend site. We note that the physiology measurements and model simulations were not done on the actual trees that died (following the papers synthesized in Adams et al., 2017) but 1 to 2 years after the major drought-induced mortality event.

2.4 | Gas exchange and water potential measurements

Gas exchange and leaf water potential measurements were performed on May 15–16, July 10–11, and August 30, 2013, at Colorado Bend, TX, USA, and on May 12–13, July 13–14, and August 28, 2013, at the Menard cave site, TX, USA. Stomatal conductance (g_s) and photosynthesis were measured with a LICOR-6400 gas exchange system (LI-COR, Lincoln, NE, USA) and leaf-to-air vapour pressure deficits (VPD_{LA}) were measured concomitantly. Data were pooled across sites for interspecies comparisons. Silhouette leaf area (i.e., projected leaf area) measured on all species using a leaf area metre (LI-3100C LI-COR, Lincoln, NE, USA) was used for calculations of gas exchange. Measurements of leaf gas exchange were performed on three to four individuals per species every 2 hr beginning at 8:00 a.m. local time and ending at approximately 5:00 p.m. local time (last measurements were initiated at 4:00 p.m. local time). Measurements on *Juniperus* were performed on shoot tips (terminal ~2 cm), which were the most recent growth of these deciduous species. Conditions in the leaf chamber were set to ambient humidity, ambient temperature, and 1,500 μmol m^{-2} s^{-1} photosynthetically active radiation (saturating light conditions).

Leaf water potential (Ψ_L) was measured using a pressure chamber (PMS Instruments, Albany, OR, USA) on the same three to four randomly selected individuals per species used for gas exchange. Leaf water potential measurements were performed at predawn and at the same time as gas exchange measurements. All measurements of gas exchange and water potential were performed on fully sun exposed south-facing shoots (except predawn). Additionally, measurements of stem water potential were performed in order to estimate (from vulnerability curves) the amount of native embolism present in stems of the measured individuals. Large disequilibria can exist between stem and leaf water potentials, especially at midday (Bucci et al., 2004). Therefore, it was necessary to bag and cover shoots (with a sealable plastic bag covered in aluminum foil) before dawn and then measure the midday water potential of bagged leaves to estimate stem water potential. Hydraulic safety margins for roots and branches were calculated as the seasonal minimum predawn water potential (for root safety margins) or the minimum branch water potential (for branch safety margins) minus the pressure inducing 50% loss of hydraulic conductivity (expressed as a negative pressure) for that particular organ. Whole-plant hydraulic safety margins and whole-plant percent loss of hydraulic conductivity were calculated from TREES (see below).

2.5 | Stem and root hydraulic properties

Branch samples of approximately 80 cm were clipped and shallow roots were excavated, traced back to their parent tree and then clipped (approximately 80 to 100 cm in length) during May 2013. Branch and root samples were immediately placed in plastic bags with wet paper towels and put into a cooler and transported back to the lab in Temple, TX, USA, approximately 2 hr away, where they were tested for open vessels (see below). To test for open vessels in branch and root segments, we used the compressed air method of Ewers and Fisher (1989), where air is forced into the proximal end of the segment at 50–100 kPa and the distal end is submerged under water. Only segments with no open vessels were used for hydraulic measurements. Following the determination of whether there were any open vessels, segments were either placed in water (at a pH of 2, to inhibit microbial growth) under a vacuum overnight or were flushed with the perfusion solution at a pressure of 50 kPa for 30 min (some samples were too long for the vacuum chamber). Maximum hydraulic conductivities were not significantly different for flushing versus vacuum (p = .41). Mean segment lengths for branches and roots (±standard error), respectively, were 46 (8.5) and 72 (10.0) cm for *Quercus*, 69 (7.6) and 102 (10.9) cm for *Prosopis*, 63 (7.5) and 87 (10.9) cm for *Diospyros*, and 23 (0.9) and 29 (2.3) cm for *Juniperus*.

To measure maximum hydraulic conductivity ($k_{h\ max}$), a hydrostatic pressure head of 6–9 kPa was used to induce flow through the segments. This pressure head was low enough to prevent refilling from occurring during measurements. The resulting volume flow rate was measured by timing the intervals for water to reach successive gradations on a pipette attached with tubing to the distal end of the segment. Branches and roots were tested for flow stability (1–2 samples per species and organ) at 15, 30, and 60 min after the initial measurements to see if any change in flow could be detected. If flows changed after 15, 30, or 60 min, then all samples of that particular organ and species were measured at the time point after which no change in flow was detected. Hydraulic conductivity (k_h) was calculated by dividing the volume flow rate of water flowing through the stem by the hydrostatic pressure gradient along the stem. Specific conductivity (k_s) was calculated by dividing k_h by the cross-sectional area

of the section being measured. The temperature of the solution was recorded before and after each specific conductivity measurement, and all conductivity calculations were corrected to 20 °C to account for changes in fluid viscosity with temperature.

Vulnerability to embolism curves were constructed using the air injection method (Sperry & Saliendra, 1994). Previous work has shown that reliable measurements of hydraulic vulnerability can be obtained by using this method even on long-vesseled species such as *Quercus*, especially when using a small pressure sleeve and ensuring there are no open vessels (Choat et al., 2010; Domec et al., 2006; Ennajeh, Simões, Khemira, & Cochard, 2011). Additionally, there has been good agreement between results using the pressure sleeve and native embolism (Domec et al., 2006). However, to ensure that there were no artifacts from using the pressure sleeve method, we resampled roots and branches of *Quercus fusiformis* (same individuals as 2013) in 2015 and measured vulnerability curves using the centrifuge method (Figure S2; Alder, Pockman, Sperry, & Nuismer, 1997; Hacke et al., 2015). Sample sizes were six each for roots and branches, and all samples were vacuumed overnight in a water (pH = 2).

For the pressure-sleeve method, after determining $k_{h\ max}$, a stem was placed in a double-ended pressure sleeve (8 cm in length) and was pressurized for 2 min. The stem was then removed from the pressure sleeve, and k_h was measured using the same method that was used for $k_{h\ max}$. This process was repeated at 0.5 or 1 MPa increments (depending on species and organ) of increasing pressure until k_h had fallen to less than 10% of its maximum value or until the upper limit of the instrument was reached (10 MPa). The percentage loss in hydraulic conductivity (PLC) was calculated as:

$$PLC = 100\times\left(1-\left(\frac{k_h}{k_{hmax}}\right)\right) \quad (1)$$

2.6 | Simulation modelling

To gain mechanistic insights on the potential causes of variability of mortality among species at our site, we employed the TREES model (Mackay et al., 2015). This plant physiology model computes soil-plant hydraulics, photosynthesis, canopy conductance (stomatal, boundary), respiration, and nonstructural carbohydrates (NSC), forced with observed meteorological data (temperature, wind speed, vapour pressure deficit, photosynthetically active radiation, and precipitation) and constrained with measured parameters on hydraulics, gas exchange, allometry, and root structure. TREES has been well tested to show that it can predict seasonal time series of water potentials, soil water content, and canopy transpiration with input of hydraulic parameters from a single day (Mackay et al., 2015; Tai et al., 2017).

We parameterized TREES with available site-specific measurements. We used half-hourly meteorological data (Lampasas 2.7 ENE, TX, USA, 30 km from Colorado Bend Field site and 153 km from Menard field site; both sites experience similar climate and water stress; see Johnson et al., 2014 and Figure S1) for the period April 1 to September 30, 2011, which was the peak of drought severity. Among the key parameters in Table S1, the hydraulic, gas exchange, and leaf area index parameters were from observations made at the study site. For leaf area, we used literature values for *Juniperus* (Hicks & Dugas, 1998), *Prosopis* (Ansley, Price, Dowhower, & Carlson, 1992; Nelson, Barnes, & Archer, 2002), *Diospyros* (Nelson et al., 2002; Rodriguez Balboa, Rodriguez, Silva, Parra, & Ramirez Lozano, 2016), and *Quercus* (Thomas, White, & Murray, 2016). The short-term simulation (April to September) did not require updating leaf area during simulation, because no new leaves were produced (or dropped), and so the role of SLA was in computing initial NSC, which was assumed to be the sum of 10% of leaf carbon, 4% of woody (stem and coarse root) carbon, and 10% of fine root carbon (Dickman, McDowell, Sevanto, Pangle, & Pockman, 2015; Sevanto et al., 2014). Respiration parameters are the same as those reported in Mackay et al. (2015).

We could not excavate the root systems for our study trees, and so we relied on a combination of evidence of rooting depth for other individuals for each species in the region (Bleby, McElrone, & Jackson, 2010; Jackson et al., 1999; McElrone et al., 2004), and fine-tuned root-depth distributions by making inferences using TREES simulations of water potentials fit to observed water potentials. *Juniperus* and *Diospyrus* have been observed to have relatively shallow roots of a few metres, whereas *Quercus* and *Prosopis* in the study site have been observed to have roots on the order of 20 m deep (Jackson et al., 1999; McElrone et al., 2004). These deeper roots contributed up to 5 times more water to transpiration than shallow roots during drought but dramatically reduced their contribution after rain (Bleby et al., 2010). In setting up simulations for each species, we adjusted the absorbing root area and depth distribution parameters until modelled predawn and midday water potentials matched the observations, but we made no adjustments to hydraulic, carbon, gas exchange, and respiration parameters. The adjusted total root depths and absorbing root area with depth are reported in Table S1.

The model was tested by comparing model output predawn and midday water potentials to measure predawn and midday water potentials in 2016 on the same individual trees as in the current study (Figure S3), which confirmed the applicability of the model to our study species. The model used half-hourly meteorological data from 2016 from the same weather station as above (Lampasas 2.7 ENE, TX, USA), and all other model parameters remained the same.

2.7 | Statistical analyses

To determine if the observed tree mortality trends were species-specific, a chi-square test of independence was conducted using R v. 3.0.2 (R Core Team, 2013). The null hypothesis was no species-specific mortality, where expected values of dead and live canopy for the chi-square test were based on total canopy cover by species and a constant mortality rate across the species. For between-species comparisons of physiological parameters, ANOVAs with post hoc Holm-Sidak comparisons were performed. Additionally, linear regressions were performed to test for significant relationships between g_s and ln VPD_{LA} and g_s and leaf water potential. An ANCOVA was performed to test for equal slopes for these relationships. ANOVA and post-hoc tests were performed using Sigmaplot 12.5 (Systat Software Inc., San Jose, CA, USA) and ANCOVA was performed using SAS 9.3 (SAS Institute Inc., Cary, NC, USA).

3 | RESULTS

3.1 | Mortality

The four-species samples represented 94% of the total canopy cover across all canopy cover loss and postdrought live cover sites (see Section 2.1). Tree canopies that were classified as dead in 2012 and 2013 imagery were observed to be dead in 2014 (Figure 1a; drought vs. postdrought). Overall, *Juniperus* had the greatest canopy dieback with 27% of sampled canopy death (Figure 1b, Table 3). Observed canopy losses for *Diospyros*, *Quercus*, and *Prosopis* were 19, 4, and 0%, respectively, and all four species were significantly different in their mortality rates (chi-square = 67.8; df = 3; $p < .0001$).

3.2 | Vulnerability to embolism and hydraulic safety margins

Vulnerability to embolism in roots and shoots varied across species (Figure 2). In general, roots were more vulnerable than branches. *Quercus* was most vulnerable to embolism having root and branch P_{50}s (pressure at which 50% of hydraulic conductivity is lost) of −1.3 and −1.8 MPa, respectively. In contrast, *Juniperus* was most resistant to embolism with a root P_{50} of −9.5 MPa and branch percent loss of conductivity was only 2% at −10 MPa, which was the limit of our instrument. *Diospyros* and *Prosopis* were intermediate in their resistance to embolism, but *Diospyros* was more resistant than *Prosopis*. All four species experienced water potentials that would result in loss of hydraulic conductivity, but to varying degrees (Figure 2). Both *Quercus* and *Prosopis* had negative safety margins, meaning that their roots and branches were predicted to lose more than 50% of hydraulic conductivity during the driest part of the field season, on the basis of vulnerability curves and measured water potentials. *Diospyros* had large, positive safety margins in roots and branches, so that even during the driest part of the season it was expected to lose little (<20%) hydraulic conductivity. *Juniperus* also had large, positive safety margins in branches and roots, such that ~99% of both branch and root conductivity was maintained throughout the study period (Figure 3a).

3.3 | Photosynthesis and stomatal sensitivity

Mean net photosynthesis during the driest month (July) was lower in *Juniperus* (1.4 μmol m^{-2} s^{-1} S.E. = 0.3, Figure 3b) than in the other species (5.0 ± 0.9, 4.9 ± 0.9, 5.4 ± 0.9 μmol m^{-2} s^{-1} in *Diospyros*, *Prosopis*, and *Quercus*, respectively). During August 2013, within 3 days after 5.0 cm of rainfall, mean net photosynthesis increased to ~11–13 μmol m^{-2} s^{-1} for *Diospyros*, *Quercus*, and *Prosopis* but remained low in *Juniperus* at 3.2 μmol m^{-2} s^{-1} (Figure S5).

Stomatal conductance (g_s) was more sensitive to changes in leaf water potential and leaf to air VPD_{LA} in *Quercus* and *Juniperus* than in *Diospyros* and *Prosopis* (Figure S4). Values of g_{S88} (the leaf water potential at which there was an 88% reduction in g_s) were similar in *Juniperus* and *Quercus*, but much more negative in *Diospyros* and *Prosopis*. Stomatal conductances at VPD_{LA} = 1 kPa ($g_{s\ ref}$) were ~60% greater in *Quercus* and *Juniperus* than in the other two species (Figure S4). The slopes of the relationships between stomatal conductance and VPD were approximately twice as great in *Quercus* and *Juniperus* as in *Diospyros* and *Prosopis*. Additionally, even when leaf water potentials were very negative (lower than −4 MPa), and VPD_{LA} was high, stomatal conductance was positive in *Diospyros* and *Prosopis*.

3.4 | Predicted NSC and modelled whole-plant loss of conductivity

TREES outputs predicted similar whole-tree NSC concentrations in all species at the end of the growing season as compared to the beginning of the growing season (Figure 4a). All species experienced increases in NSC in the middle of the growing season and a decline late in the season. Predicted year-end NSC concentrations were 5.5%, 6.5%, 4.8%, and 5.8% in *Juniperus*, *Diospyros*, *Quercus*, and *Prosopis*, respectively. All species in the study were predicted to have large losses of whole-plant hydraulic conductance (Figure 4b). *Juniperus* was predicted to have spent 95% of the growing season at a whole-plant percentage loss of conductance (PLC) of greater than 60% (Figure S7). Predicted amounts of time at PLC greater than 60% were not as large in the other species as compared to *Juniperus*, but they were still quite high; 61% of the time in *Diospyros*, 48% of the time in *Quercus*, and 57% in *Prosopis*.

TABLE 3 Tree canopy cover loss due to the 2011 drought in the Edward's Plateau region—A summary of 21 plots

	Dead canopy cover (m)		Live canopy cover (m)	
Species[1] (mortality rate)	Observed	Expected	Observed	Expected
Juniperus ashei (27%)* ↑	224	172	610	662
Quercus fusiformis (4%)* ↓	12	58	271	225
Diospyros texana (19%)	17	19	73	71
Other less common species[2] (15%)	13	17	71	67
Chi-square = 67.8; df = 3, $p < .0001$				

[1]Species ordered by percent abundance (total cover).

[2]Species, with canopy cover less than 2% of the total, were aggregated to avoid small expected values. These species include: *Prosopis glandulosa*, *Sideroxylon lanuginosum*, *Acacia roemeriana*, *Ulmus crassifolia*, *Condalia hookeri*, *Celtis laevigata var. reticulata*, *Aloysia gratissima*, *Mahonia trifoliolata*, *Rhus lanceolata*, *Opuntia engelmannii*, *Acacia farnesiana*, and *Celtis laevigata*.

*Significant positive (↑) and negative (↓) differences from expected dead canopy values (chi-square test, for each species compared to sum of all others, df = 1, $p < .0001$). Expected values were based on total canopy cover by species and assumed a constant mortality rate across the species.

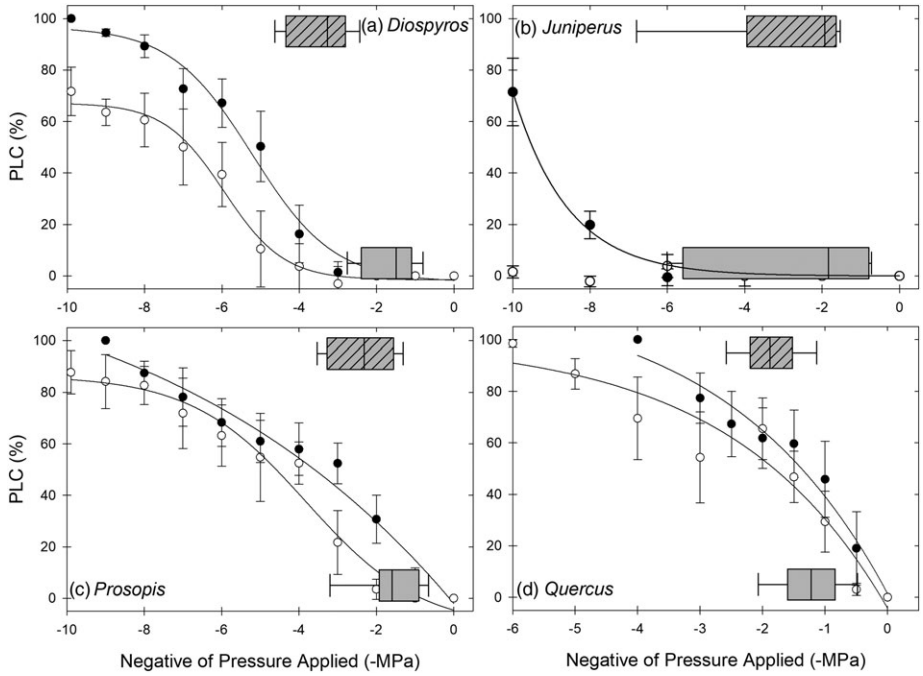

FIGURE 2 Embolism vulnerability curves for four co-occurring Texas species. Closed symbols are roots and open symbols are branches. Horizontal boxplots indicate range of predawn leaf (lower unhatched) and midday branch (upper hatched) water potentials measured over the summer of 2013 and include the 25th to 75th percentiles. Vertical lines within boxes represent median values and vertical lines outside of boxes represent 10th and 90th percentiles of measured values

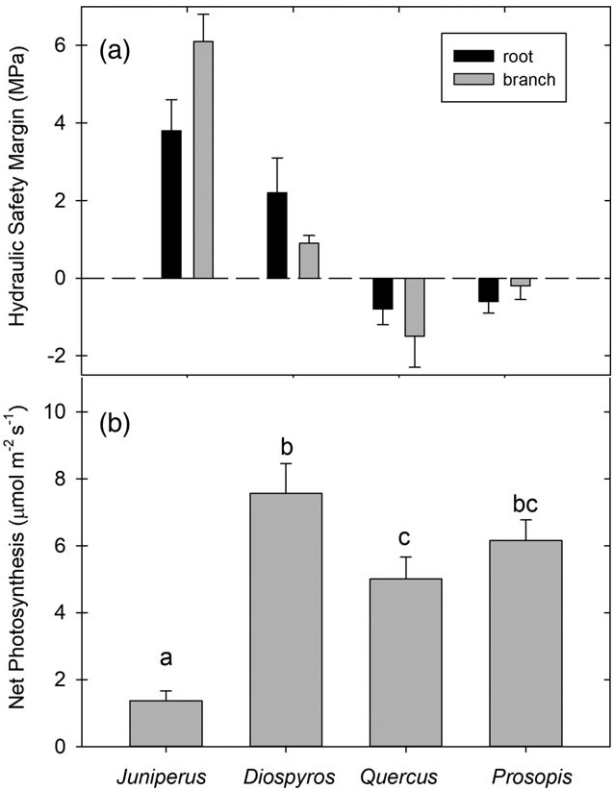

FIGURE 3 Root and branch hydraulic safety margins (a, Ψ_{min}–P_{50}). Safety margins were calculated as the minimum seasonal predawn leaf or midday branch water potential minus the root or branch P_{50}, respectively. Panel b is net photosynthesis during the driest month (July). Error bars are standard errors around the P_{50} measurements in Panel a and standard errors in Panel b. Different letters in Panel b represent significant differences

3.5 | Water use envelope, relative hydraulic safety, and belowground conductance

The mean seasonal water use envelope corresponding to the upper boundary for water transport and expressed as $E_{CRIT} - E_C$ (E_{CRIT} is the modelled transpiration at which the hydraulic system is predicated to fail and E_C is the modelled transpiration), was smaller in the species with greater mortality (*Juniperus* and *Diospyros*) than in the species with little or no mortality (*Quercus* and *Prosopis*; Figure 5a,b). By the end of the growing season, the water use envelope was predicted to be near zero in *Diospyros* (0.46 mmol m^{-2} s^{-1}) and below 1 mmol m^{-2} s^{-1} in *Juniperus* (0.94 mmol m^{-2} s^{-1}) but greater than 1 mmol m^{-2} s^{-1} in *Quercus* and *Prosopis* (1.47 and 2.48 mmol m^{-2} s^{-1}, respectively). Additionally, the proportion of maximum water use envelope at the end of the growing season was 0.05 and 0.07 in *Juniperus* and *Diospyros*, respectively, but was 0.17 and 0.23 in *Quercus* and *Prosopis*. The predicted relative hydraulic safety expressed as $(E_{CRIT} - E_C)/\max(E_{CRIT} - E_C)$ was lowest in the two species with the greatest observed mortality (Figure 6). Plotted as a function of the average soil water potential experienced by the entire plant rooting volume, the near-zero values of relative hydraulic safety in *Juniperus* and *Diospyros* were associated with more negative soil water potentials.

Modelled belowground hydraulic conductance declined in all species across the growing season (Figure 7). However, the decline in conductance early in the season was much greater in *Diospyros* and *Juniperus* than in *Quercus* or *Prosopis*, and this reduced conductance persisted throughout the season. Additionally, by the end of the season, modelled belowground hydraulic conductance was lower in *Diospyros* and *Juniperus* (0.33 and 0.60 mmol m^{-2} s^{-1} MPa^{-1}, respectively) than in *Quercus* or *Prosopis* (0.94 and 0.88 mmol m^{-2} s^{-1} MPa^{-1}, respectively).

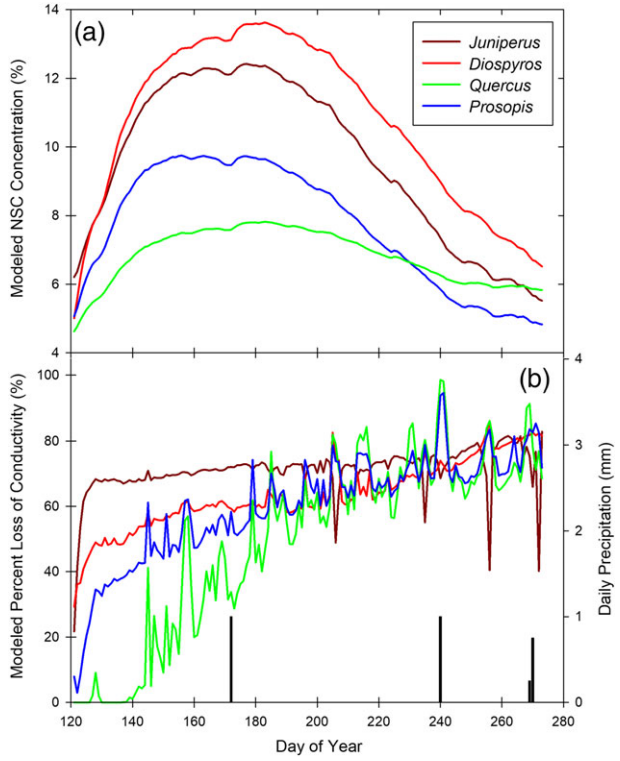

FIGURE 4 TREES simulated whole-tree nonstructural carbohydrate (NSC) concentrations (a) and whole-tree percent loss of hydraulic conductivity (b) between May 1 and September 30, 2011. Vertical bars in Panel b represent daily precipitation in 2011

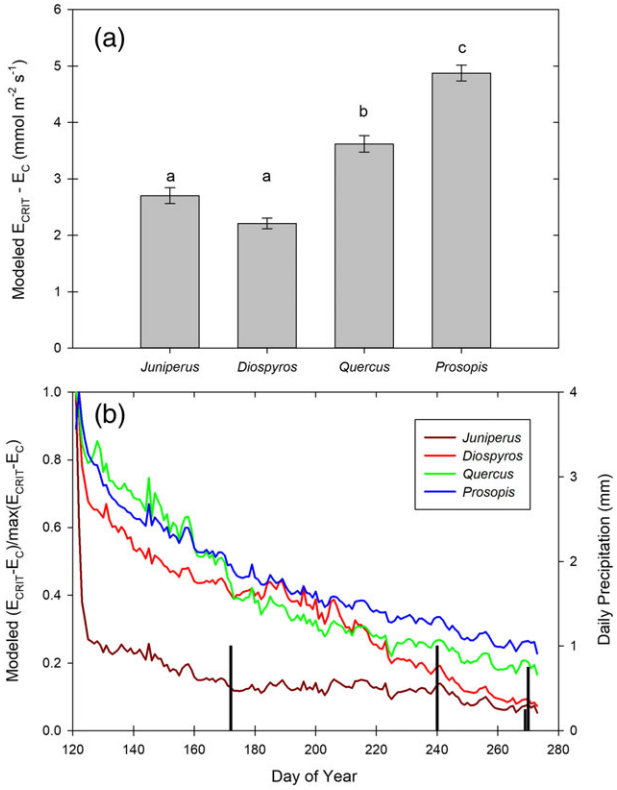

FIGURE 5 (a) Mean difference between critical (E_{CRIT}) and actual (E_C) transpiration as predicted by the TREES model for 2011. Different letters indicate significant differences (ANOVA $p < .001$, post-hoc Tukey's). Error bars are standard errors. (b) Seasonal changes in difference between critical (E_{CRIT}) and actual (E_C) transpiration as predicted by the TREES model. Vertical bars in Panel b represent daily precipitation in 2011

3.6 | Isohydry and hydraulic safety margins

The species in this study clumped into two groups when applying a framework of stomatal regulation of xylem embolism versus hydraulic safety margin (Figure 8). Species that experienced greater mortality (i.e., *Juniperus* and *Diospyros*) were grouped into a quadrant where hydraulic safety margins (calculated from branch and root measurements) were positive and stomatal closure limited water potentials such that estimated embolism levels did not reach 50% PLC. *Quercus* and *Prosopis* had negative safety margins and stomata that allowed water potentials to reach values that caused xylem loss of conductivity to exceed 50%.

Branch and whole-tree hydraulic safety margins (whole-tree safety margin calculated as $\Psi_{soil\ min}$ − modelled whole tree P_{50}) were similar in *Quercus* (−1.5 and −1.0 MPa, respectively) but were not similar in the other species (Figure 9). Branch safety margin was −0.2 MPa in *Prosopis*, whereas whole-tree safety margin was −1.8 MPa. In *Diospyros*, branch and whole-tree safety margins were 0.9 and −4.5 MPa, respectively. The difference between branch and whole-tree safety margin was greatest in *Juniperus*, where branch safety margin was 6.1 MPa and whole-tree safety margin was −5.4 MPa.

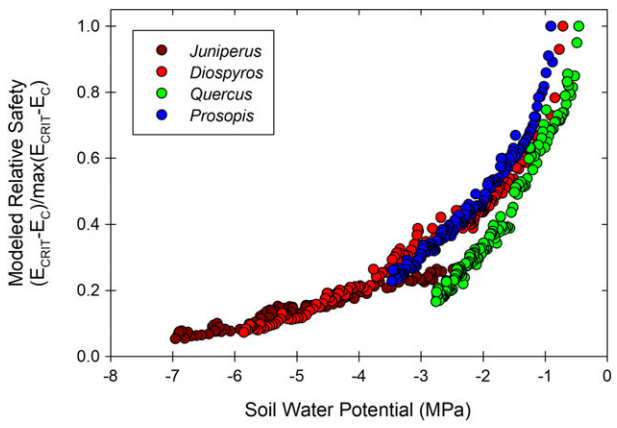

FIGURE 6 TREES simulated relative hydraulic safety as expressed as (E_{CRIT} − E_C)/max(E_{CRIT} − E_C) versus the mean soil water potential experienced by the entire rooting volume for 2011

4 | DISCUSSION

During the most severe drought in recorded history in central Texas, we found that patterns of drought-induced tree mortality were best explained by belowground hydraulic decline as predicted from TREES, a highly constrained and whole-tree mechanistic model. This was indicated by losses in modelled belowground hydraulic conductance (Figure 7) and reductions in the water use envelope (Figure 5) despite no concomitant reductions in branch and root xylem conductivity (Figures 2 and 3a). Many previously used metrics to predict or to

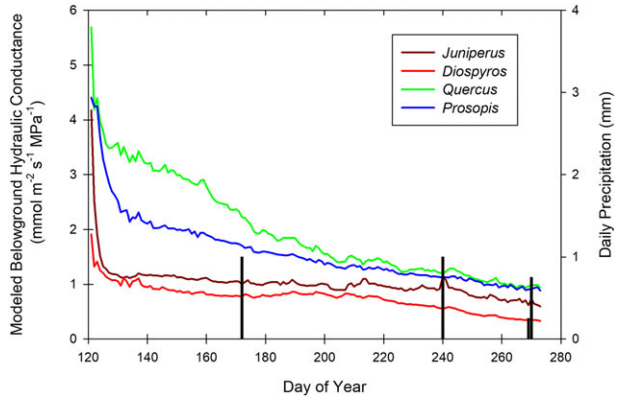

FIGURE 7 TREES simulated total belowground hydraulic conductance between May 1 and September 30, 2011. Vertical bars in Panel b represent daily precipitation in 2011

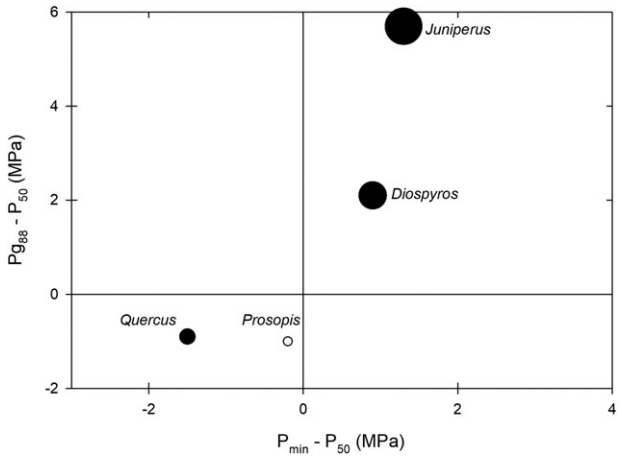

FIGURE 8 The degree of stomatal regulation of embolism ($P_{g88} - P_{50}$) versus hydraulic safety margin ($P_{min} - P_{50}$). Each symbol size is representative of the percent observed mortality for each species (with open symbol representing no mortality in *Prosopis glandulosa*)

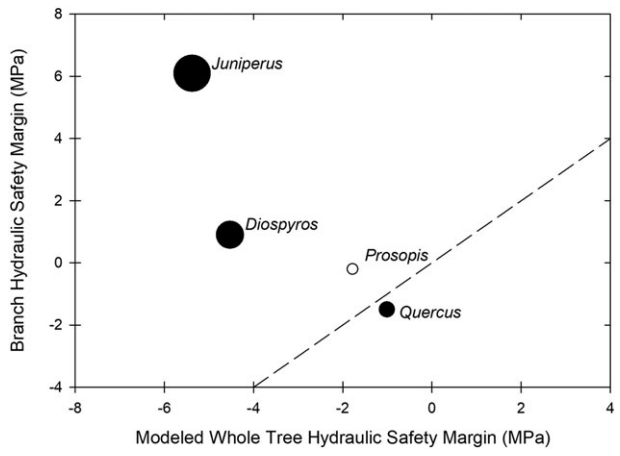

FIGURE 9 Branch hydraulic safety margin versus whole-tree hydraulic safety margin. Branch hydraulic safety margin was calculated as minimum branch water potential minus branch P_{50} and whole-tree hydraulic safety margin was calculated as mean minimum soil water potential experienced by the entire rooting volume minus whole tree P_{50} (see Figure S7). Each symbol size is representative of the percent observed mortality for each species (with open symbol representing no mortality in *Prosopis glandulosa*)

determine the mechanism of drought-induced mortality were not related to mortality in our study system, including the degree of iso/anisohydry, depending on how it was defined (Figure 8, also see text below), organ-level hydraulic safety margins (Figure 3a), photosynthesis (Figure 3b), and carbohydrate depletion (Figure 4). Further, the species that have been observed having deeper roots (Jackson et al., 1999) were the species with the least mortality.

Juniperus suffered the greatest mortality and this is consistent with a major drought that occurred in the 1950s where *Juniperus* also had high mortality (Young, 1956). Likely due to changes in fire regimes, *Juniperus* has been encroaching into areas previously dominated by live oak savannas (Taylor et al., 2012). The 2011–2013 drought and future droughts could serve to prevent the encroachment of *Juniperus* into areas where it has not been abundant in the past. It is likely that *Juniperus* is the most sensitive to drought of these species due to more shallow rooting depths than the other co-occurring species (Jackson et al., 1999), as predicted from the more negative predawn water potentials than the other species (Table 2, Figure 2). It is also possible that recent colonization of *Juniperus* has been in less favourable sites than those already occupied by *Quercus*, *Prosopis*, and *Diospyros*, and those less favourable sites have thinner soils or other characteristics that allow them to dry more quickly during drought. Using analyses of tree rings and other approaches, Polley, Johnson, and Jackson (2016) showed that *Juniperus ashei* trees growing more slowly before the drought were disproportionately vulnerable to mortality during the drought and this may have reflected individuals growing in less favourable sites.

4.1 | Proposed mechanisms not consistent with observed mortality

Hydraulic safety margins and xylem hydraulic failure has been related to drought-induced plant mortality in both gymnosperm and angiosperm tree species (e.g., Adams et al., 2017; Anderegg et al., 2012; Anderegg et al., 2016; Brodribb & Cochard, 2009; Nardini, Battistuzzo, & Savi, 2013; Urli et al., 2013). *Juniperus* was the species in this study with the most embolism-resistant xylem, and *Quercus* was the species with the least resistant xylem (Figure 2), but *Juniperus* had high mortality and *Quercus* had very little. Further, the species in this study with negative branch and root safety margins experienced little or no mortality but maintained higher whole plant conductivity. Conversely, the species with the greatest branch and root safety margins experienced the greatest mortality. Therefore, hydraulic safety margins based on branch and root vulnerability curves may not be a useful predictor of mortality in some systems.

The degree of isohydry in combination with hydraulic safety margins has also been used as a predictor of drought-induced plant mortality (McDowell et al., 2008; Skelton et al., 2015). Previous studies have predicted that plants that had negative safety margins and were relatively anisohydric should die from hydraulic failure more quickly during drought. In our study, *Juniperus* and *Diospyros* had positive safety margins and were relatively isohydric (Figures 3a and 8), and they had the greatest mortality. *Quercus* and *Prosopis*, the species with negative safety margins and anisohydric stomatal function had little or no mortality. Discrepancies between our observed mortality and that

predicted by some frameworks focusing on degree of isohydry may be attributable to the extent to which whole-tree hydraulic vulnerability is taken into consideration (Johnson et al., 2016); as opposed to that of a single organ, such as branches. It should be noted, however, that using a more recent definition of isohydry (hydroscape area, Meinzer et al., 2016), these species would be categorized differently with *Juniperus* and *Diospyros* being more anisohydric and *Quercus* and *Prosopis* being on the more isohydric end of the spectrum (Johnson et al., 2018). In that case, the degree of isohydry would be more consistent with the observed patterns of mortality. Due to multiple metrics for isohydry that are often contrasting (e.g., Martínez-Vilalta & Garcia-Forner, 2017), the outcome of drought mortality for "isohydric" plants depends on which metric was chosen to describe the degree of isohydry. In fact, some recent papers have called for rethinking the isohydric concept altogether (Garcia-Forner et al., 2016; Martínez-Vilalta & Garcia-Forner, 2017). We chose to use the framework of Skelton et al. (2015), because it expressly predicts mortality mechanisms based on their definition of isohydry.

Carbon imbalance has been another reported cause of plant mortality during droughts. Certainly, hydraulic losses can result in reduced carbon gain via stomatal closure, so by no means is death from carbon imbalance or hydraulic failure mutually exclusive. Reductions in NSC during drought have been associated with mortality (Adams et al., 2013; Mitchell et al., 2013). However, in our current study, all species had very similar modelled NSC concentrations at the end of the growing season (Figure 4a). These values of NSC should, however, be considered approximate due to interlab variability (Quentin et al., 2015). Also, although photosynthesis was lowest in *Juniperus* during the driest month of the study (Figure 2c), photosynthesis was greatest over this period in *Diospyros*, a species that also experienced high mortality. Neither measured nor modelled carbon relations provided a reliable predictor for mortality.

4.2 | Mechanisms explaining observed mortality

We found that modelled belowground hydraulic conductance (and the resulting modelled whole-plant conductance) was the best predictor of mortality in the current study. This was indicated by the predicted whole tree percent loss of conductance, the water use envelope and predicted belowground hydraulic conductance (Figures 4b, 5, 6, and 7). *Juniperus* spent 95% of the growing season with greater than 60% loss of whole plant hydraulic conductance (Figures 4b and S7). This result is consistent with prior studies that have suggested that time spent above PLC of ~60% is a good predictor of mortality (Adams et al., 2017; McDowell et al., 2013; Sperry & Love, 2015). However, rather than experience this PLC in the branches or roots, the large loss of conductivity in this study appeared to occur below ground in locations or tissues other than coarse roots. Possible explanations for how this belowground hydraulic conductance would decline in situ are either declines in soil hydraulic conductivity, mechanical failure (i.e., roots no longer in contact with soil particles), hydraulic failure of fine root cortical cells or fine root embolism upon exposure to drying soil (Cuneo, Knipfer, Brodersen, & McElrone, 2016).

Whole-tree safety margins, calculated from whole plant hydraulic conductance, were also consistent with the observed patterns of mortality (Figure 9), whereas branch and root safety margins were not. Branch and root safety margins may not be a good indicator of whole plant function in general. For example, we found as much as an 11.5 MPa difference between whole plant and branch-based safety margins in *Juniperus*. Further, a recent study using an additive hydraulic resistance approach found that differences in whole tree and branch P_{50} values were similarly as large: 12.6 MPa in *Juniperus ashei* and up to a 3.2 MPa difference in other species (Johnson et al., 2016).

4.3 | Rooting depth and belowground hydraulic failure

Rooting depth has been explored extensively as an ecological strategy for tree survival in water-limited ecosystems (Canadell et al., 1996; Johnson et al., 2014; Schenk & Jackson, 2002; Schulze et al., 1996), with tree species observed having remarkably deep roots in many arid and semiarid systems (>50 m). Recent studies have called for a better understanding of belowground processes and their implementation in process-based models for improving our ability to predict drought-induced tree mortality (McDowell et al., 2013; Phillips et al., 2016).

In the current study, *Quercus* and *Prosopis* are known to have much deeper roots than either *Juniperus* or *Diospyros* (Jackson et al., 1999). Bleby et al. (2010), for instance, showed that deep roots of *Quercus* and *Prosopis* contributed up to 5 times more water to transpiration than shallow roots during drought but dramatically reduced their contributions after rain. The potential importance of relatively deep rooting was also supported by *Prosopis* and *Quercus* having less negative water potentials than either *Juniperus* or *Diospyros* (Table 2, Figures 2, S8), and simulations of such water potentials were only possible with deep roots (20 m or deeper) included in the model for *Prosopis* and *Quercus*. It is possible that the mortality patterns observed here are due primarily to differences in rooting depth, which impacted belowground hydraulic conductance. The range of rooting depths in the current study may not be common in many ecosystems and maximum rooting depth can vary greatly within an ecosystem type (e.g., Canadell et al., 1996). In areas with more shallowly rooted species, the physiological frameworks that we found to be consistent with tree mortality need to be evaluated for their ability to be predictive of drought induced mortality.

4.4 | Other drought-related agents resulting in tree mortality

Plant mortality can occur from factors other than carbon imbalance and hydraulic dysfunction during drought. Biotic agents and fire can cause extensive tree mortality during drought periods (Dale et al., 2001; Negrón, McMillin, Anhold, & Coulson, 2009; Raffa et al., 2008) and multiple fires were observed during the 2011–2013 Texas drought (Schwantes et al., 2016). It should be noted that we intentionally chose sites for this study that had not burned, and we observed no insect damage on any of the trees in our study sites. Still, microbial agents cannot be ruled out as contributing to the mortality of these trees.

Another potential causative factor that was not measured in this study is phloem dysfunction. Recently, reductions in phloem transport capacity have been predicted during periods of drought (Woodruff, 2013; Sevanto et al., 2014). Empirical evidence of radial flow between xylem and phloem (Sevanto, Hölttä, & Holbrook, 2011), synthesis across species (Mencuccini, Minunno, Salmon, Martínez-Vilalta, & Hölttä, 2015), and modelling (Hölttä, Mencuccini, & Nikinmaa, 2009) suggest that loss of phloem transport is mediated by changes in osmotic potential under moderate drought but inhibited during extreme drought due to high viscosity. Such high viscosity can be associated with high concentrations of NSC (Figure 3) under low relative water use envelopes (Figure S6).

It should also be noted that the measurements of physiology of trees in this study were on individuals that had survived the drought. It is possible that the drought killed susceptible individuals that were different in some way (e.g., allometrically, age, rooted in different soils, or soil layers) from the surviving individuals. This is a caveat of this type of study where measurements are made postdrought and inference is made to what happened during the drought.

With near-future droughts likely becoming both more frequent and more intense (Diffenbaugh et al., 2015; IPCC, 2013; Trenberth et al., 2014) the need for improved understanding of drought responses of trees across ecosystems is critical and urgent. A greater mechanistic understanding of drought responses will improve process models of drought-induced forest mortality, aid land managers in determining species selection and stocking densities, and even allow for estimates of changes in forest ecosystem services (e.g., water outputs for downstream irrigation of agriculture). Snapshots of plant function, such as plant functional traits, even though they are easy to collect and widely available in the literature, are unlikely to yield mechanistic information that will be useful moving forward. Instead, a more holistic, even multidisciplinary approach (Abrams & Nowacki, 2016) looking at whole plant physiological functioning will likely yield the most useful data and conclusions.

ACKNOWLEDGMENTS

This work was funded by USDA-AFRI (#2012-00857), NSF IOS-1146746, NSF IOS-1549971, and NSF EAR-1344703. N. G. M. was supported by the Department of Energy, Office of Science and Laboratory Directed Research and Development support from PNNL. D. S. M. was supported by the National Science Foundation through grant IOS-1450679. K. A. M. was supported by the National Science Foundation grant IOS-1557906. We thank Philip Fay, Chris Kolodziejczyk, Katherine Jones, Anne Gibson, and Kyle Tiner for assistance in coordination of field campaigns. The authors would also like to thank Josiah Strauss, Ashley Brasovan, and Will Cook for field assistance.

AUTHOR CONTRIBUTIONS

D. M. J., J-C. D., D. S. M., N. G. M., and R. B. J. designed the study. All authors contributed to data collection, analysis and writing of the manuscript. The authors have no conflict of interest.

ORCID

Daniel M. Johnson http://orcid.org/0000-0003-1015-9560

REFERENCES

Abrams, M. D., & Nowacki, G. J. (2016). An interdisciplinary approach to better assess global change impacts and drought vulnerability on forest dynamics. *Tree Physiology*, *36*, 421–427.

Adams, H. D., Germino, M. J., Breshears, D. D., Barron-Gafford, G. A., Guardiola-Claramonte, M., Zou, C. B., & Huxman, T. E. (2013). Non-structural leaf carbohydrate dynamics of Pinus edulis during drought-induced tree mortality reveal role for carbon metabolism in mortality mechanism. *New Phytologist*, *197*, 1142–1151.

Adams, H. D., Zeppel, M. J., Anderegg, W. R., Hartmann, H., Landhäusser, S. M., Tissue, D. T., … McDowell, N. G. (2017). A multi-species synthesis of physiological mechanisms in drought-induced tree mortality. *Nature Ecology and Evolution*, in press.

Alder, N. N., Pockman, W. T., Sperry, J. S., & Nuismer, S. (1997). Use of centrifugal force in the study of xylem cavitation. *Journal of Experimental Botany*, *48*, 665–674.

Allen, C. D., Breshears, D. D., & McDowell, N. G. (2015). On underestimation of global vulnerability to tree mortality and forest die-off from hotter drought in the Anthropocene. *Ecosphere*, *6*, 1–55.

Anderegg, W. R., Berry, J. A., Smith, D. D., Sperry, J. S., Anderegg, L. D., & Field, C. B. (2012). The roles of hydraulic and carbon stress in a widespread climate-induced forest die-off. *Proceedings of the National Academy of Sciences*, *109*, 233–237.

Anderegg, W. R., Klein, T., Bartlett, M., Sack, L., Pellegrini, A. F., Choat, B., & Jansen, S. (2016). Meta-analysis reveals that hydraulic traits explain cross-species patterns of drought-induced tree mortality across the globe. *Proceedings of the National Academy of Sciences*, *113*, 5024–5029.

Ansley, R. J., Price, D. L., Dowhower, S. L., & Carlson, D. H. (1992). Seasonal trends in leaf area of honey mesquite trees: Determination using image analysis. *Journal of Range Management*, *45*, 339–344.

Auken, O. W., Ford, A. L., Stein, A., & Stein, A. G. (1980). Woody vegetation of upland communities in the southern Edwards Plateau. *Texas Journal of Science*, *32*, 25–35.

Beerling D. (2008) *The emerald planet: How plants changed Earth's history*. OUP Oxford.

Bleby, T. M., McElrone, A. J., & Jackson, R. B. (2010). Water uptake and hydraulic redistribution across large woody root systems to 20 m depth. *Plant Cell Environment*, *33*, 2132–2148.

Brodribb, T. J., & Cochard, H. (2009). Hydraulic failure defines the recovery and point of death in water-stressed conifers. *Plant Physiology*, *149*, 575–584.

Bucci, S. J., Scholz, F. G., Goldstein, G., Meinzer, F. C., Hinojosa, J. A., Hoffmann, W. A., & Franco, A. C. (2004). Processes preventing nocturnal equilibration between leaf and soil water potential in tropical savanna woody species. *Tree Physiology*, *24*, 1119–1127.

Canadell, J., Jackson, R. B., Ehleringer, J. B., Mooney, H. A., Sala, O. E., & Schulze, E. D. (1996). Maximum rooting depth of vegetation types at the global scale. *Oecologia*, *108*, 583–595.

Choat, B., Drayton, W. M., Brodersen, C., Matthews, M. A., Shackel, K. A., Wada, H., & McElrone, A. J. (2010). Measurement of vulnerability to water stress-induced cavitation in grapevine: A comparison of four techniques applied to a long-vesseled species. *Plant, Cell & Environment*, *33*, 1502–1512.

Choat, B., Jansen, S., Brodribb, T. J., Cochard, H., Delzon, S., Bhaskar, R., … Zanne, A. E. (2012). Global convergence in the vulnerability of forests to drought. *Nature*, *491*, 752–755.

Core Team, R. (2013). *R: A language and environment for statistical computing*. Vienna, Austria: R Foundation for Statistical Computing.

Cuneo, I. F., Knipfer, T., Brodersen, C. R., & McElrone, A. J. (2016). Mechanical failure of fine root cortical cells initiates plant hydraulic decline during drought. *Plant Physiology*, *172*, 1669–1678.

Dale, V. H., Joyce, L. A., McNulty, S., Neilson, R. P., Ayres, M. P., Flannigan, M. D., … Simberloff, D. (2001). Climate change and forest disturbances: Climate change can affect forests by altering the frequency, intensity,

duration, and timing of fire, drought, introduced species, insect and pathogen outbreaks, hurricanes, windstorms, ice storms, or landslides. *Bioscience*, *51*, 723–734.

Dickman, L. T., McDowell, N. G., Sevanto, S., Pangle, R. E., & Pockman, W. T. (2015). Carbohydrate dynamics and mortality in a piñon-juniper woodland under three future precipitation scenarios. *Plant, Cell & Environment*, *38*, 729–739.

Diffenbaugh, N. S., Swain, D. L., & Touma, D. (2015). Anthropogenic warming has increased drought risk in California. *Proceedings of the National Academy of Sciences*, *112*, 3931–3936.

Domec, J.-C., Scholz, F. G., Bucci, S. J., Meinzer, F. C., Goldstein, G., & Villalobos-Vega, R. (2006). Diurnal and seasonal variation in root xylem embolism in neotropical savanna woody species: Impact on stomatal control of plant water status. *Plant, Cell & Environment*, *29*, 26–35.

Ennajeh, M., Simões, F., Khemira, H., & Cochard, H. (2011). How reliable is the double-ended pressure sleeve technique for assessing xylem vulnerability to cavitation in woody angiosperms? *Physiologia Plantarum*, *142*, 205–210.

Ewers, F. W., & Fisher, J. B. (1989). Techniques for measuring vessel lengths and diameters in stems of woody plants. *American Journal of Botany*, *76*, 645–656.

Garcia-Forner, N., Adams, H. D., Sevanto, S., Collins, A. D., Dickman, L. T., Hudson, P. J., … McDowell, N. G. (2016). Responses of two semiarid conifer tree species to reduced precipitation and warming reveal new perspectives for stomatal regulation. *Plant, Cell & Environment*, *39*, 38–49.

Griffin, D., & Anchukaitis, K. J. (2014). How unusual is the 2012–2014 California drought? *Geophysical Research Letters*, *41*, 9017–9023.

Hacke, U. G., Venturas, M. D., MacKinnon, E. D., Jacobsen, A. L., Sperry, J. S., & Pratt, R. B. (2015). The standard centrifuge method accurately measures vulnerability curves of long-vesselled olive stems. *New Phytologist*, *205*, 116–127.

Hicks, R. A., & Dugas, W. A. (1998). Estimating ashe juniper leaf area from tree and stem characteristics. *Journal of Range Management*, *51*, 633–637.

Hölttä, T., Mencuccini, M., & Nikinmaa, E. (2009). Linking phloem function to structure: Analysis with a coupled xylem–phloem transport model. *Journal of Theoretical Biology*, *259*, 325–337.

IPCC (2013). *Climate change 2013: The physical science basis. Working Group I contribution to the Fifth assessment report of the Intergovernmental Panel on climate change*. Cambridge, UK: Cambridge University Press.

Jackson, R. B., Moore, L. A., Hoffmann, W. H., Pockman, W. T., & Linder, C. R. (1999). Ecosystem rooting depth determined with caves and DNA. *Proceedings of the National Academy of Sciences, USA*, *96*, 11387–11392.

Johnson, D. M., Sherrard, M. E., Domec, J.-C., & Jackson, R. B. (2014). Role of aquaporin activity in regulating deep and shallow root hydraulic conductance during extreme drought. *Trees*, *28*, 1323–1331.

Johnson, D. M., Wortemann, R., McCulloh, K. A., Jordan-Meille, L., Ward, E., Warren, J. M., … Domec, J.-C. (2016). A test of the hydraulic vulnerability segmentation hypothesis in conifer and angiosperm tree species. *Tree Physiology*, *36*, 383–393.

Johnson, D. M., Berry, Z. C., Baker, K. V., Smith, D. D., McCulloh, K. A., & Domec, J.-C. (2018). Leaf hydraulic parameters are more plastic in species that experience a wider range of leaf water potentials. *Functional Ecology* (in press).

Kolb, K. J., & Davis, S. D. (1994). Drought tolerance and xylem embolism in co-occurring species of coastal sage and chaparral. *Ecology*, *75*, 648–659.

Kukowski, K. R., Schwinning, S., & Schwartz, B. F. (2013). Hydraulic responses to extreme drought conditions in three co-dominant tree species in shallow soil over bedrock. *Oecologia*, *171*, 819–830.

Linton, M. J., Sperry, J. S., & Williams, D. G. (1998). Limits to water transport in *Juniperus osteosperma* and *Pinus edulis*: Implications for drought tolerance and regulation of transpiration. *Functional Ecology*, *12*, 906–911.

Mackay, D. S., Roberts, D. E., Ewers, B. E., Sperry, J. S., McDowell, N. G., & Pockman, W. T. (2015). Interdependence of chronic hydraulic dysfunction and canopy processes can improve integrated models of tree response to drought. *Water Resources Research*, *51*, 6156–6176.

Martínez-Vilalta, J., & Garcia-Forner, N. (2017). Water potential regulation, stomatal behaviour and hydraulic transport under drought: Deconstructing the iso/anisohydric concept. *Plant, Cell & Environment*, *40*, 962–976.

McDowell, N. G. (2011). Mechanisms linking drought, hydraulics, carbon metabolism, and vegetation mortality. *Plant Physiology*, *155*, 1051–1059.

McDowell, N. G., & Allen, C. D. (2015). Darcy's law predicts widespread forest mortality under climate warming. *Nature Climate Change*, *5*, 669–672.

McDowell, N. G., Fisher, R. A., Xu, C., Domec, J.-C., Hölttä, T., Mackay, D. S., … Limousin, J. M. (2013). Evaluating theories of drought-induced vegetation mortality using a multimodel–experiment framework. *New Phytologist*, *200*, 304–321.

McDowell, N. G., Pockman, W. T., Allen, C. D., Breshears, D. D., Cobb, N., Kolb, T., … Yepez, E. A. (2008). Mechanisms of plant survival and mortality during drought: Why do some plants survive while others succumb to drought? *New Phytologist*, *178*, 719–739.

McElrone, A. J., Pockman, W. T., Martinez-Vilalta, J., & Jackson, R. B. (2004). Variation in xylem structure and function in stems and roots of trees to 20 m depth. *New Phytologist*, *163*, 507–517.

Meinzer, F. C., Johnson, D. M., Lachenbruch, B., McCulloh, K. A., & Woodruff, D. R. (2009). Xylem hydraulic safety margins in woody plants: Coordination of stomatal control of xylem tension with hydraulic capacitance. *Functional Ecology*, *23*, 922–930.

Meinzer, F. C., Woodruff, D. R., Marias, D. E., Smith, D. D., McCulloh, K. A., Howard, A. R., & Magedman, A. L. (2016). Mapping 'hydroscapes' along the iso-to anisohydric continuum of stomatal regulation of plant water status. *Ecology Letters*, *19*, 1343–1352.

Mencuccini, M., Minunno, F., Salmon, Y., Martínez-Vilalta, J., & Hölttä, T. (2015). Coordination of physiological traits involved in drought-induced mortality of woody plants. *New Phytologist*, *208*, 396–409.

Mitchell, P. J., O'Grady, A. P., Tissue, D. T., White, D. A., Ottenschlaeger, M. L., & Pinkard, E. A. (2013). Drought response strategies define the relative contributions of hydraulic dysfunction and carbohydrate depletion during tree mortality. *New Phytologist*, *197*, 862–872.

Moore, G. W., Edgar, C. B., Vogel, J. G., Washington-Allen, R. A., March, R. G., & Zehnder, R. (2016). Tree mortality from an exceptional drought spanning mesic to semiarid ecoregions. *Ecological Applications*, *26*, 602–611.

Nardini, A., Battistuzzo, M., & Savi, T. (2013). Shoot desiccation and hydraulic failure in temperate woody angiosperms during an extreme summer drought. *New Phytologist*, *200*, 322–329.

Negrón, J. F., McMillin, J. D., Anhold, J. A., & Coulson, D. (2009). Bark beetle-caused mortality in a drought-affected ponderosa pine landscape in Arizona, USA. *Forest Ecology & Management*, *257*, 1353–1362.

Nelson, J. A., Barnes, P. W., & Archer, S. (2002). Leaf demography and growth responses to altered resource availability in woody plants of contrasting leaf habit in a subtropical savanna. *Plant Ecology*, *160*, 193–205.

O'Brien, M. J., Leuzinger, S., Philipson, C. D., Tay, J., & Hector, A. (2014). Drought survival of tropical tree seedlings enhanced by non-structural carbohydrate levels. *Nature Climate Change*, *4*, 710–714.

Oren, R., Sperry, J. S., Katul, G. G., Pataki, D. E., Ewers, B. E., Phillips, N., & Schäfer, K. V. R. (1999). Survey and synthesis of intra-and interspecific variation in stomatal sensitivity to vapour pressure deficit. *Plant, Cell & Environment*, *22*, 1515–1526.

Padilla, F. M., & Pugnaire, F. I. (2007). Rooting depth and soil moisture control Mediterranean woody seedling survival during drought. *Functional Ecology*, *21*, 489–495.

Phillips, R. P., Ibanez, I., D'Orangeville, L., Hanson, P. J., Ryan, M. G., & McDowell, N. G. (2016). A belowground perspective on the drought sensitivity of forests: Towards improved understanding and simulation. *Forest Ecology & Management*, *380*, 309–320.

Pinheiro, H. A., DaMatta, F. M., Chaves, A. R., Loureiro, M. E., & Ducatti, C. (2005). Drought tolerance is associated with rooting depth and stomatal control of water use in clones of *Coffea canephora*. *Annals of Botany*, *96*, 101–108.

Polley, H. W., Briske, D. D., Morgan, J. A., Wolter, K., Bailey, D. W., & Brown, J. R. (2013). Climate change and North American rangelands: Trends, projections, and implications. *Rangeland Ecology and Management*, *66*, 493–511.

Polley, H. W., Johnson, D. M., & Jackson, R. B. (2016). Canopy foliation and area as predictors of mortality risk from episodic drought for individual trees of Ashe juniper. *Plant Ecology*, *217*, 1105–1114.

Quentin, A. G., Pinkard, E. A., Ryan, M. G., Tissue, D. T., Baggett, L. S., Adams, H. D., … Woodruff, D. R. (2015). Non-structural carbohydrates in woody plants compared among laboratories. *Tree Physiology*, *35*, 1146–1165.

Raffa, K. F., Aukema, B. H., Bentz, B. J., Carroll, A. L., Hicke, J. A., Turner, M. G., & Romme, W. H. (2008). Cross-scale drivers of natural disturbances prone to anthropogenic amplification: The dynamics of bark beetle eruptions. *Bioscience*, *58*, 501–517.

Rodriguez Balboa, P. C., Rodriguez, H. G., Silva, I. C., Parra, A. C., & Ramirez Lozano, R. G. (2016). Leaf morphological traits of then shrub species at the Tamaulipan thorn scrub. *International Journal of Bio-Resource & Stress Management*, *7*, 344–349.

Schenk, H. J., & Jackson, R. B. (2002). Rooting depths, lateral root spreads and below-ground/above-ground allometries of plants in water-limited ecosystems. *Journal of Ecology*, *90*, 480–494.

Schulze, E. D., Mooney, H. A., Sala, O. E., Jobbagy, E., Buchmann, N., Bauer, G., … Ehleringer, J. R. (1996). Rooting depth, water availability, and vegetation cover along an aridity gradient in Patagonia. *Oecologia*, *108*, 503–511.

Schwantes, A. M., Swenson, J. J., González-Roglich, M., Johnson, D. M., Domec, J.-C., & Jackson, R. B. (2017). Measuring canopy loss and climatic thresholds from an extreme drought along a 5-fold precipitation gradient across Texas. *Global Change Biology*, (online early view) doi: https://doi.org/10.1111/gcb.13775.

Schwantes, A. M., Swenson, J. J., & Jackson, R. B. (2016). Quantifying drought-induced tree mortality in the open canopy woodlands of central Texas. *Remote Sensing of Environment*, *181*, 54–64.

Sevanto, S., Hölttä, T., & Holbrook, N. M. (2011). Effects of the hydraulic coupling between xylem and phloem on diurnal phloem diameter variation. *Plant, Cell & Environment*, *34*, 690–703.

Sevanto, S., McDowell, N. G., Dickman, L. T., Pangle, R., & Pockman, W. T. (2014). How do trees die? A test of the carbon starvation hypothesis. *Plant, Cell & Environment*, *37*, 153–161.

Skelton, R. P., West, A. G., & Dawson, T. E. (2015). Predicting plant vulnerability to drought in biodiverse regions using functional traits. *Proceedings of the National Academy of Sciences*, *112*, 5744–5749.

Sperry, J. S., Adler, F. R., Campbell, G. S., & Comstock, J. C. (1998). Limitation of plant water use by rhizosphere and xylem conductances: Results from a model. *Plant, Cell & Environment*, *21*, 347–359.

Sperry, J. S., & Love, D. M. (2015). Tansley review: What plant hydraulics can tell us about plant responses to climate-change droughts. *New Phytologist*, *207*, 14–27.

Sperry, J. S., & Saliendra, N. Z. (1994). Intra- and inter-plant variation in xylem cavitation in *Betula occidentalis*. *Plant, Cell & Environment*, *17*, 1233–1241.

Tai, X., Mackay, D. S., Anderegg, W. R. L., Sperry, J. S., & Brooks, P. D. (2017). Plant hydraulics improves and topography mediates prediction of aspen mortality in southwestern USA. *New Phytologist*, *213*, 113–127.

Tardieu, F., & Simonneau, T. (1998). Variability among species of stomatal control under fluctuating soil water status and evaporative demand: Modelling isohydric and anisohydric behaviours. *Journal of Experimental Botany*, *49*, 419–432.

Taylor Jr, C. A., Twidwell, D., Garza, N. E., Rosser, C., Hoffman, J. K., & Brooks, T. D. (2012). Long-term effects of fire, livestock herbivory removal, and weather variability in Texas semiarid savanna. *Rangeland Ecology & Management*, *65*(1), 21–30.

Thomas, J. A., White, J. D., & Murray, D. B. (2016). Tree species influence woodland canopy characteristics and crown fire potential. *Forest Ecology & Management*, *362*, 169–176.

Thurow T.L. & Hester J.W. (1997) How an increase or reduction in Juniper cover alters rangeland hydrology. *Juniper Ecology and Management 1997 Symposium Proceedings*.

Trenberth, K. E., Dai, A., van der Schrier, G., Jones, P. D., Barichivich, J., Briffa, K. R., & Sheffield, J. (2014). Global warming and changes in drought. *Nature Climate Change*, *4*, 17–22.

Urli, M., Porté, A. J., Cochard, H., Guengant, Y., Burlett, R., & Delzon, S. (2013). Xylem embolism threshold for catastrophic hydraulic failure in angiosperm trees. *Tree Physiology*, *33*, 672–683.

Willson, C. J., Manos, P. S., & Jackson, R. B. (2008). Hydraulic traits are influenced by phylogenetic history in the drought-resistant, invasive genus *Juniperus* (Cupressaceae). *American Journal of Botany*, *95*, 299–314.

Woodruff, D. R. (2013). The impacts of water stress on phloem transport in Douglas-fir trees. *Tree Physiology*, *34*, 5–14.

Young, V. A. (1956). The effect of the 1949-1954 drought on the ranges of Texas. *Journal of Range Management*, *9*, 139–142.

SUPPORTING INFORMATION

Additional Supporting Information may be found online in the supporting information tab for this article.

How to cite this article: Johnson DM, Domec J-C, Carter Berry Z, et al. Co-occurring woody species have diverse hydraulic strategies and mortality rates during an extreme drought. *Plant Cell Environ*. 2018;1–13. https://doi.org/10.1111/pce.13121